

IEICE Proceeding Series

Frequency-Modulated Time-Delayed Microwave Chaotic Oscillator

Hien Dao, John C. Rodgers, Thomas E. Murphy, Rajarshi Roy

Vol. 1 pp. 670-673

Publication Date: 2014/03/17

Online ISSN: 2188-5079

Downloaded from www.proceeding.ieice.org

Frequency-Modulated Time-Delayed Microwave Chaotic Oscillator

Hien Dao^{1,2}, John C. Rodgers², Thomas E. Murphy^{2,3}, and Rajarshi Roy^{4,5}

1. Chemical Physics Graduate Program
 2. Institute for Research in Electronics and Applied Physics
 3. Department of Electrical and Computer Engineering
 4. Institute for Physical Science and Technology
 5. Department of Physics
- University of Maryland, College Park, MD 20742 USA
 Email: hiendao@umd.edu

Abstract—We report a chaotic frequency-modulated (FM) microwave source with time-delayed feedback. The system supports dynamical behaviors ranging from periodic to high-dimensional chaos, depending on the feedback gain and filter bandwidth. The experimental implementation uses both microwave and digital components to achieve the nonlinearity and time-delayed feedback, respectively. We discuss the possible applications in range and velocity sensing.

1. Introduction

Since the 1950s, chaos has developed into a new science because of its universality and applicability. The fact that a chaotic signal is complex and noise-like makes it an ideal candidate for communication and ranging applications. One can think of employing chaotic signals in sensor networks to provide security when transferring information [1, 2]. The short correlation time of chaotic signals can be useful in applications that require random signal generation [3]. Chaos also can have a wide bandwidth, which is useful for increased precision of transmitted signals in radar and sonar systems [4]. After being introduced by Ikeda in [5], the time delayed feedback loop has proved to be an effective method to produce chaos in many experimental systems such as laser systems [6] and electronics circuit [7]. The chaotic signals produced by these systems are examples of *amplitude chaos*, i.e., a signal with an irregular time-varying amplitude or envelope. However, for some applications in communication, it is preferable to use *phase chaos*, in which the chaotic signal has a constant amplitude and a chaotic phase or frequency.

Because most communication and ranging systems using microwave frequencies, a chaotic system operates in this regime is of considerable interest for practical applications. Although there are many classical electrical circuits that can produce broadband chaotic waveforms, it is difficult to scale these systems to the microwave frequencies because in high speed systems

the time delay associated with signal propagation is often non-negligible in comparison to the dynamical timescales.

In this paper, we describe a microwave FM chaotic oscillator with a time-delayed feedback loop. This architecture can take advantage of the unavoidable signal propagation delays in electronic systems. The high-speed FM chaotic signal could also offer advantages such as low probability of detection or interception in radar systems, reduced interference with existing channels, and less susceptibility to noise or jamming than normal transmitted signals in sensor networks.

2. Microwave Time-delayed Feedback Loop

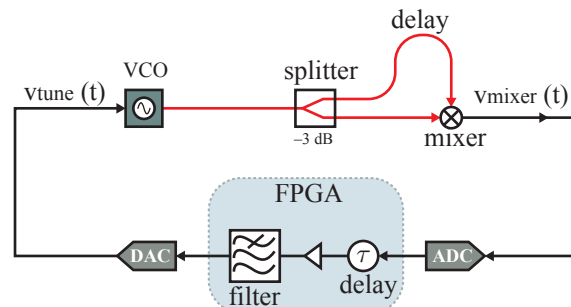


Figure 1: Experimental system used to produce chaotic frequency-modulated microwave signals. The system uses a conventional microwave voltage-controlled oscillator (VCO) with a self-homodyne microwave frequency discriminator to produce a sinusoidal nonlinearity. The output is then fed back to the input through a time-delayed lowpass filter.

The microwave system shown in Fig. 1 uses commercially available devices with a time-delayed feedback architecture to produce chaotic microwave signals. The nonlinear function of the system is produced by a conventional voltage-controlled oscillator

(VCO) and a self-homodyne microwave frequency discriminator comprising a splitter, a microwave cable and a double-balanced mixer. The VCO is a FM device which produces a constant-amplitude microwave signal whose frequency varies linearly with the applied voltage v_{tune} . The signal generated by the VCO is split into two identical copies, one of which is delayed with respect to the other through the microwave cable. These two phase-modulated signals are then sent to the input ports of the mixer to provide a baseband output signal, v_{mixer} , which is a sinusoidal function of frequency of the VCO. With the exception of the microwave delay line, which was constructed using a small coil of semirigid coaxial cable, all elements of the nonlinearity were soldered onto a printed circuit board and interconnected with microstrip waveguides designed to have a 50Ω impedance. Fig. 2 plots the experimentally measured sinusoidal relationship between the tuning voltage v_{tune} and the mixer output v_{mixer} , together with a best-fit sinusoid. From these measurements, one can determine the two constants: an amplitude $A = 0.2$ V and the voltage needed to make 2π phase shift, $V_{2\pi} = 0.5$ V. The deviation from a perfect sinusoidal nonlinearity is attributed to small, non-ideal dependence of the VCO power on the applied voltage v_{tune} .

The time delay and lowpass filter were implemented digitally using a programmable logic board (Altera Cyclone FPGA). The delay time corresponds to the length of a digital shift register while the filter function was obtained by programming a discrete-time filter. The input to the FPGA was obtained by an 8-bit analog to digital converter, sampled at 75 Ms/s, and the output was likewise provided by a synchronously sampled 10-bit digital-to-analog converter. The critical parameters of the system, such as the filter time-constant, signal delay time and feedback gain could be conveniently adjusted through re-programming the FPGA.

As indicated in Fig. 2, output of the mixer may be described by

$$v_{\text{mixer}}(t) = A \cos \left(2\pi \frac{v_{\text{tune}}(t)}{v_{2\pi}} + \phi_0 \right) \quad (1)$$

where the factor A is related to the loop gain and microwave power and the phase ϕ_0 is determined by the offset frequency of the VCO (i.e., the VCO frequency when $v_{\text{tune}} = 0$.)

The lowpass filter and time delay in the feedback loop can be modeled by the simple first-order differential equation,

$$\tau_{\text{lpf}} \frac{d}{dt} v_{\text{tune}}(t) + v_{\text{tune}} = v_{\text{mixer}}(t - \tau) \quad (2)$$

where the τ_{lpf} denotes the time-constant of the lowpass filter and τ is the feedback time delay. Taken together,

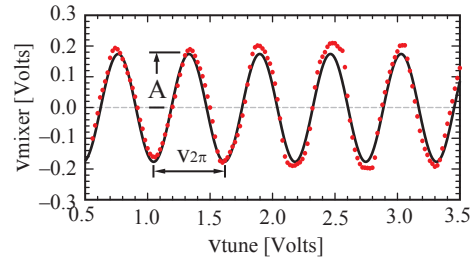


Figure 2: Experimentally measured relationship between the input v_{tune} and output v_{mixer} for a VCO followed by a self-homodyne frequency discriminator comprising a 10 ns microwave delay line and a mixer. The solid curve indicates the best-fit sinusoidal function. From these measurements, one can determine the two constants $A = 0.2$ V and $v_{2\pi} = 0.5$ V, as shown.

the tuning voltage can be described by the following first-order delay differential equation:

$$\tau_{\text{lpf}} \frac{dv_{\text{tune}}}{dt} + v_{\text{tune}} = A \cos \left(2\pi \frac{v_{\text{tune}}(t - \tau)}{v_{2\pi}} + \phi_0 \right) \quad (3)$$

This equation can be re-cast in terms of the normalized dimensionless amplitude x , defined as

$$x(t) \equiv 2\pi \frac{v_{\text{tune}}(t)}{v_{2\pi}} \quad (4)$$

and the time variable t may be likewise normalized in terms of the round-trip delay time τ . This in turn gives the normalized delay differential equation:

$$a \frac{d}{dt} x(t) = -x(t) + \beta \cos [x(t - 1) + \phi_0] \quad (5)$$

where t is now understood to represent the dimensionless time (measured in units of τ), and the two dimensionless constants R and a are defined by

$$\beta \equiv 2\pi \frac{A}{v_{2\pi}}, \quad a \equiv \frac{\tau_{\text{lpf}}}{\tau} \quad (6)$$

For the measurements reported here, the lowpass filter was designed to have a cutoff frequency of 1.35 MHz, which corresponds to a time-constant of $\tau_{\text{lpf}} = 118$ ns. The feedback delay was adjusted to $\tau = 1$ μ s, so that $a = 0.118$. The phase offset was held constant at $\phi_0 = -\pi/2$, while the gain β was adjusted by programming the FPGA.

3. The Route to Chaos

In addition to experimental observations, (5) was numerically integrated to study the dynamical behavior. Following the method of Farmer [8], we divide the time delay into small discrete time-steps, which allows

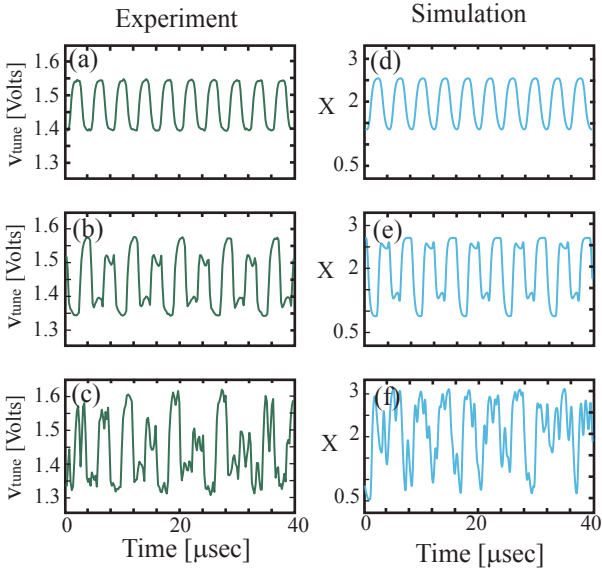


Figure 3: Time evolution of the system observed experimentally (left) and simulated numerically (right) as the feedback strength β is varied. $\beta = 2.4$ (a,d), $\beta = 2.7$ (b,e), $\beta = 3$ (c,f)

the delay differential equation to be approximated by a discrete-time vector map equation that can be easily and efficiently solved.

As the feedback gain increases, the dynamics of the system varies from steady state and oscillatory, to quasiperiodic to chaotic. Fig. 3 shows typical experimentally observed and numerically simulated, time traces of the input of the VCO, v_{tune} , for three choices of feedback strength β . For $\beta < 2.3$, the system has a fixed point solution which is stable, and at $R = 2.3$, the stable fixed point undergoes a Hopf bifurcation into a periodic state with an approximate period of 4τ (0.25 MHz), as shown in Fig. 3(a,d). The amplitude of $x(t)$ also increases with the feedback gain. At $\beta = 2.65$ the system again enters a quasi-periodic state in which the period is 2τ (0.5 MHz), as in Fig. 3(b,e). As the feedback strength is further increased, the system undergoes a series of period-doubling bifurcations, eventually leading to chaos. For $\beta > 3$, both simulation and experiment show irregular, aperiodic behavior, as depicted in Fig. 3(c,f).

The route to chaos is further illustrated by bifurcation diagrams and the calculation of the maximum Lyapunov exponent of the system shown in Fig. 4. The bifurcation diagram (both experimental and simulated) was obtained by constructing a color scale histogram of characteristic time traces as the feedback strength β was smoothly increased from 2.3 to 3.5. The simulated and observed bifurcation diagrams are qualitatively similar, and while the precise locations of bifurcation points do not exactly match, all of the rele-

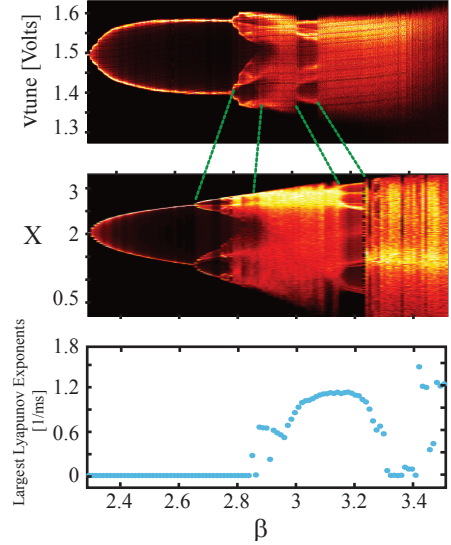


Figure 4: Bifurcation diagrams of the system are constructed by using a color histogram functions on time traces as the feedback strength β is smoothly varied from 2.3 to 3.5. (a) Experimental data from the 8-bit oscilloscope, (b) Numerical data from Matlab, (c) Largest Lyapunov exponents calculated by solving linearized system equation.

vant dynamical behaviors are observed in each region.

The lower panel of Fig. 4 shows the calculated largest Lyapunov exponent of the system, obtained by linearizing Eq. 5 about its dynamical state. The regions with positive Lyapunov exponent confirm the existence of chaos in the system. For the time traces shown in Fig. 3(c,f), the calculated Lyapunov exponent is 0.715 (1/ms). When the VCO is modulated by this chaotic signal, the resulting RF signal is an aperiodic frequency-modulated signal, i.e., *phase chaos*.

4. Chaotic FM Radar

Chaotic FM microwave signals could potentially find applications in ranging and radar systems, which could benefit from the broadband noise-like nature of the signal. The aperiodicity of a chaotic FM signal can provide lower probability of detection or interception and reduces the susceptibility to interference from/with other microwave channels.

To compare the effectiveness in target detection, we compute the ambiguity function of the microwave chaotic signal:

$$\chi(\tau, f) = \int_{-\infty}^{+\infty} s(t)s^*(t - \tau)e^{-i2\pi f\tau} dt \quad (7)$$

where $s(t)$ is the frequency-modulated microwave sig-

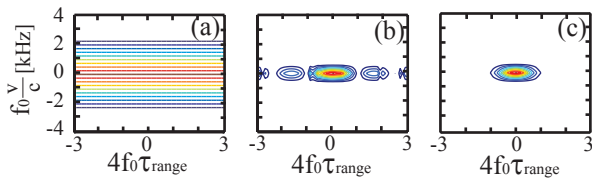


Figure 5: The calculated ambiguity functions of the continuous waveform (a), a periodic FM signal (b) and a chaotic FM signal (c). The function is calculated using Fourier transform with center frequency f_0 on complex signals as velocity and the range of the target are varied.

nal,

$$s(t) = \exp\left(i2\pi\gamma \int v_{\text{tune}}(t)dt\right) \quad (8)$$

and γ is the tuning coefficient of the VCO (typically given in MHz/V).

The ambiguity function is a two-dimensional function of τ and f , which represent time-delay and Doppler shift of the reflected signal, respectively. The ambiguity function provides information about how well a matched receiver can unambiguously measure the range (τ) and velocity (f) of a signal.

Fig. 5 shows a contour plot of the magnitude $|\chi(\tau, f)|$, illustrating the advantages of using a chaotic FM signal in range and velocity sensing. Fig. 5a was obtained by using a continuous-wave microwave signal (i.e., $v_{\text{tune}} = \text{constant}$), for which the range cannot be unambiguously determined, as expected. Fig. 5b was obtained using a periodic v_{tune} , in which case the Doppler shift (f) can be more accurately estimated, and the position can also be determined. Because the modulation is periodic (with a period of approximately $4 \mu\text{s}$), the range can only be determined up to an additive integral multiple of $4 \mu\text{s}$. Fig. 5c was obtained using a larger feedback strength, for which the modulation is chaotic. In this case, the system is predicted to yield more precise and unambiguous measurement of both range and velocity.

5. Conclusion

We demonstrated a microwave time-delayed feedback loop utilizing both microwave and digital components. The dynamics of the loop can be modeled by a time delay differential equation. We discussed the route to chaos of the system with a first order lowpass filter by showing characteristic time traces along with bifurcation diagrams. The numerical results agreed with the experimentally observed data. The existence of chaos in the system was proven with the calculation of the Lyapunov exponents. We also numerically considered the advantages of the chaotic FM signal in

radar and ranging applications by calculating the ambiguity function, showing the improvement on performance that can be obtained through the use of chaotic FM waveforms.

Acknowledgments

This work was funded by DOD MURI Grant No. ONR N000140710734.

References

- [1] G. Mykolaitis, A. Tamasevicius, A. Cenys, S. Bumeliene, A. N. Anagnostopoulos, and N. Kalkan, "Very High and Ultrahigh Frequency Hyper-chaotic Oscillator with Delay Line," *Chaos Solitons Fractal*, vol. 17, pp. 343–347, 2003.
- [2] J. N. Blakely, L. Illing, and D. J. Gauthier, "High-Speed Chaos in an Optical Feedback System with Flexible Timescales," *IEEE J. Quantum Electron*, vol. 40, pp. 299–305, 2004.
- [3] J. T. Gleeson, "Truly Random Number Generator Based on Turbulent Electro-Convection," *Appl. Phys. Lett.*, vol. 81, p. 1949, 2002.
- [4] K. Myneni, T. A. Barr, B. R. Reed, S. D. Pethel, and N. J. Corron, "High-Precision Ranging using Chaotic Laser Pulse Train," *Appl. Phys. Lett.*, vol. 74, pp. 1496–1498, 2001.
- [5] K. Ikeda and K. Matsumoto, "High-dimensional Chaotic Behaviors in Systems with Time-delayed Feedback," *Physica D*, vol. 29, pp. 223–235, 1987.
- [6] A. B. Cohen, B. Ravoori, T. E. Murphy, and R. Roy, "Using Synchronization for Prediction of High-Dimensional Chaotic Dynamics," *Phys. Rev. Lett.*, vol. 101, p. 154102, 2008.
- [7] L. Illing and D. J. Gauthier, "Ultra-high-frequency Chaos in a Time-delay Electronic Device with Band-Limited Feedback," *Chaos*, vol. 16, p. 033119, 2006.
- [8] J. D. Farmer, "Chaotic Attractors of an Infinite-dimensional Dynamical System," *Physica D*, vol. 4, no. 3, pp. 366–393, 1982.